Water Research X 24 (2024) 100252

Contents lists available at ScienceDirect

Water Research X

journal homepage: www.sciencedirect.com/journal/water-research-x

A cohesive *Microcoleus* strain cluster causes benthic cyanotoxic blooms in rivers worldwide

Pilar Junier [a,#,##], Guillaume Cailleau [a], Mathilda Fatton [a], Pauline Udriet [a], Isha Hashmi [a], Danae Bregnard [a], Andrea Corona-Ramirez [a], Eva di Francesco [a], Thierry Kuhn [a], Naïma Mangia [a], Sami Zhioua [a], Daniel Hunkeler [b], Saskia Bindschedler [a], Simon Sieber [c,##,$], Diego Gonzalez [a,##,*]

[a] *Laboratory of Microbiology, University of Neuchâtel, Switzerland*
[b] *Centre for Hydrogeology and Geothermics, University of Neuchâtel, Switzerland*
[c] *Department of Chemistry, University of Zürich, Switzerland*

ARTICLE INFO

Keywords:
Anatoxin-a
Benthic cyanobacteria
Microcoleus anatoxicus
Cyanobacterial blooms

ABSTRACT

Over the last two decades, proliferations of benthic cyanobacteria producing derivatives of anatoxin-a have been reported in rivers worldwide. Here, we follow up on such a toxigenic event happening in the Areuse river in Switzerland and investigate the diversity and genomics of major bloom-forming riverine benthic cyanobacteria. We show, using 16S rRNA-based community profiling, that benthic communities are dominated by Oscillatoriales. We correlate the detection of one *Microcoleus* sequence variant matching the *Microcoleus anatoxicus* species with the presence of anatoxin-a derivatives and use long-read metagenomics to assemble complete circular genomes of the strain. The main dihydro-anatoxin-a-producing strain in the Areuse is distinct from strains isolated in New Zealand, the USA, and Canada, but forms a monophyletic strain cluster with them with average nucleotide identity values close to the species threshold. Compared to the rest of the *Microcoleus* genus, the toxin-producing strains encode a 15 % smaller genome, lacking genes for the synthesis of some essential vitamins. Toxigenic mats harbor a distinct microbiome dominated by proteobacteria and bacteroidetes, which may support cyanobacterial growth by providing them with essential nutrients. We recommend that strains closely related to *M. anatoxicus* be monitored internationally in order to help predict and mitigate similar cyanotoxic events.

Introduction

Cyanobacterial blooms pose a significant threat to aquatic ecosystems and human health. Many cyanobacteria produce toxic metabolites, collectively called cyanotoxins, which are active against a wide range of potential competitors and predators, from bacteria to vertebrates (Carpine and Sieber, 2021; Janssen, 2019; Mehinto et al., 2021; Paerl and Otten, 2013; Quiblier et al., 2013; Sieber et al., 2020). Because of their potency and wide target-range, these toxins can profoundly affect the functioning of ecosystems (Svirčev et al., 2019; Zanchett and Oliveira-Filho, 2013). Cyanotoxins also represent a direct danger for human health when people are exposed to them during recreational activities or through drinking water; in addition, some cyanotoxins are able to bioaccumulate along the trophic chain, potentially building up in fish or meat (Ferrão-Filho and Kozlowsky-Suzuki, 2011).

While a majority of reported blooms are caused by cyanobacteria proliferating in the water column, blooms of substrate-attached, i.e. benthic, species are increasingly documented (McAllister et al., 2016; Puddick et al., 2022; Quiblier et al., 2013; Wood et al., 2020). Benthic blooms typically originate as thick mats on the bed of rivers and lakes; through the action of shearing forces or in response to an internal developmental program, the mats can detach from the substrate and accumulate at the surface (McAllister et al., 2016). Benthic blooms are associated with many different toxins, but most commonly with

* Corresponding author at: Rue Emile-Argand 11, CH-2000, Neuchatel, Switzerland.
E-mail addresses: pilar.junier@unine.ch (P. Junier), simon.sieber@uzh.ch (S. Sieber), diego.gonzalez@unine.ch (D. Gonzalez).
[#] Pilar Junier, Rue Emile-Argand 11, CH-2000, Neuchatel, Switzerland; +41 32 718 22 44.
[##] contributed equally
[$] Simon Sieber, Winterthurerstrasse 190, CH-8057, Zürich, Switzerland

https://doi.org/10.1016/j.wroa.2024.100252
Received 23 March 2024; Received in revised form 21 August 2024; Accepted 27 August 2024
Available online 4 September 2024

anatoxin-a (ATX) and its congeners, homoanatoxin-a (HTX), dihydroanatoxin-a (dhATX), and dihydrohomoanatoxin-a (dhHTX) (Wood et al., 2020); all are potent agonists of the nicotinic acetylcholine receptors present in the nervous system of many vertebrates (Colas et al., 2021). ATX-producing benthic blooms have been reported from all over the world, including in European rivers and lakes, e.g. the rivers La Loue and Le Tarn in France and Lech in Germany, as well as the lake Tegel in Germany (Bauer et al., 2020; Cadel-Six et al., 2007; Fastner et al., 2018; Gugger et al., 2005). Such blooms have been particularly well documented in New Zealand, in the USA, and more recently in Canada (Bouma-Gregson et al., 2018; Colas et al., 2021; Conklin et al., 2020; Heath et al., 2011; McAllister et al., 2018; Thomson-Laing et al., 2020; Valadez-Cano et al., 2023; Wood et al., 2020, 2018), where they are caused by strains belonging to the *Microcoleus* genus (Oscillatioriales) (Strunecký et al., 2013; Tee et al., 2021).

Partial, fragmented genomes have been assembled for several ATX-producing benthic strains isolated in New Zealand, the USA, and Canada (Conklin et al., 2020; Tee et al., 2021; Valadez-Cano et al., 2023). Toxigenic strains from the three countries are closely related at the nucleotide level and have common genomic features compared to other *Microcoleus* strains, in particular a smaller genome size and missing genes in common vitamin biosynthetic pathways (Tee et al., 2021). Among them, only one species has been properly described, *Microcoleus anatoxicus* Stancheva & Conklin, whose type strain is PTRS2 from the Russian river in the USA (Bouma-Gregson et al., 2019; Conklin et al., 2020). How the sequenced *Microcoleus* strains from New Zealand and Canada relate to the *M. anatoxicus* species is not entirely clear and the overall genetic diversity of ATX-congener synthesizing *Microcoleus* strains is unknown.

Here, we explore the diversity of ATX-producing benthic cyanobacterial strains in the Areuse, a river flowing into the Lake Neuchâtel on the Swiss plateau. We use microbial community profiling and metagenomics to identify the strains responsible for toxin production and to survey the diversity of benthic cyanobacteria in the river. While ATX-associated blooms and deaths of dogs have been reported in many rivers and lakes in Europe, this is the first such event that is fully documented both at the microbial community composition and at the genomic levels.

Results

A cyanotoxic event associated with the proliferation of a Microcoleus strain

By the end of July 2020, six dogs died <24 h after being in contact with cyanobacterial floating mats close to the mouth of the river Areuse at the shore of the Lake Neuchâtel (Switzerland). The toxicological analyses performed on the dogs identified anatoxin-a (ATX), a widespread toxin of cyanobacterial origin, as the most likely cause of death. This prompted us to investigate the cyanobacterial diversity associated with benthic mats in several locations along the Areuse (Fig. 1A).

We first sampled the floating mats, which accumulated at the mouth of the river right after the toxigenic event (Fig. 1BC). These mats were mostly composed of filamentous cyanobacteria resembling Oscillatoriales (Fig. 1DE). The closest matches of the dominant cyanobacterial 16SrRNA gene amplicons were Oscillatoriales belonging to the *Microcoleus* genus or related basonyms (STable 1). To determine the full bacterial community composition, we used high-throughput 16S rRNA gene amplicon (V3-V4 region) sequencing on two initial samples (7cyano2 and 7cyano1). These were largely dominated by one *Microcoleus* amplicon sequence variant (ASV) representing >65 % of the bacterial reads in both samples (Fig. 1FGH). *Microcoleus* species common in rivers of temperate countries are known to synthesize anatoxin-a derivatives (Conklin et al., 2020; Kelly et al., 2018). Our data therefore suggested that a *Microcoleus* strain capable of producing anatoxin-a congeners was proliferating in the Areuse.

Geographic origin, distribution, and diversity of blooming strains

To know more about the distribution of the toxigenic strains along the river Areuse, we took multiple samples of cyanobacterial mats and biological material growing on immersed rocks, wood or sediments at three main locations along the river (Fig. 1A, SFigure 1): in the delta on the river bed (11 samples, both mats and sediments; STable 1), on the banks along the last 1 km of the river (23 samples, both floating mats and sediments; STable 1), and at a dam located five kilometers upstream of the mouth, close to the village of Noiraigue (7 samples, floating mats only; STable 1). Floating mats were only observed near the mouth of the river and in Noiraigue. At the mouth of the river, the bed was almost entirely covered in dark photosynthetic microbial mats (SVideo 1), which were mostly absent on the lake floor (SVideo 2). A distinct type of floating cyanobacterial mats, whose color was bright green, was also collected in the lower part of the Areuse (samples 34, X, Y1 and Y2; some pictures and micrographs in SFigure 1).

To analyze the bacterial community composition, we performed high-throughput 16S rRNA gene amplicon sequencing (V3-V4 region) on DNA extracted from these samples. Filamentous cyanobacteria were largely dominant in floating mats (up to 85 % of reads) and well represented in sediments (usually min. 20 % of reads) (Fig. 2AB). Among cyanobacteria, *Microcoleus* dominated most samples, while *Potamolinea* dominated samples 34, X, Y1, Y2. The *Microcoleus* genus included a significant diversity with at least 20 different ASVs present across samples. One of these ASVs, identified as *Microcoleus anatoxicus* (Conklin et al., 2020), was dominant in the floating mats sampled in the delta and in the upper Areuse (Noiraigue).

In parallel, we used published primers targeting the *anaC* gene to test samples for the presence of the ATX biosynthesis cluster (Kelly et al., 2018). While virtually all the samples from the delta tested positive, the marker was only detected in a quarter of the samples from other parts of the Areuse (STable 1). This suggests that, while it is sporadically present all along the river, the ATX producing strain only reached high densities in the delta region.

The presence of ATX and dhATX was confirmed by analyzing the samples by ultra-high-performance liquid chromatography (UHPLC) coupled with a high-resolution mass spectrometer (HR-MS) (Müller et al., 2022) or a triple quadrupole mass spectrometer (TQMS) (Turner et al., 2022). The extract from floating mats dominated by *Microcoleus* contained 0.1 % and 3 % of ATX and dhATX respectively (1.4 μg / mg of ATX-a and 29.4 μg / mg of dhATX, calculated on extract dry weight); in these samples, ATX and dhATX amounted to approximately 0.003 % and 0.07 % of dry algal biomass respectively. In contrast, the extract of the samples dominated by *Potamolinea* contained <0.03 % of dhATX (0.26 μg / mg of dhATX, calculated on extract dry weight) and ATX was undetectable.

Genetic relatedness of ATX-producing Microcoleus strains worldwide

All samples that tested positive for *anaC* contained a significant proportion of the *Microcoleus anatoxicus* ASV. To know more about the genomics of these strains, we used a long-read high-throughput sequencing technology (Pacific Biosciences SMRT) to sequence DNA extracted from four samples (A, N, 600, and X). For all four samples, we obtained a number of large contigs that were binned based on coverage and tetranucleotide identity, and classified based on global homology and full 16S rRNA gene sequences (Fig. 3A, SFigures 2–5, STable 2). We were able to assemble the full circular genome of a *Microcoleus* strain for sample A and N, as well as large contigs of a *Microcoleus* strain for sample 600 and large contigs of a *Potamolinea* strain for sample X. As expected, the contigs assembled from sample X (*Potamolinea* sp.) belonged to a different branch of the cyanobacterial phylogenetic tree, clustering with Coleofasciculates close to Nostocales (SFigure 6).

The full *Microcoleus* genomes assembled from samples A and N (hereafter strain NeuA) were very close (>99.99 % average nucleotide

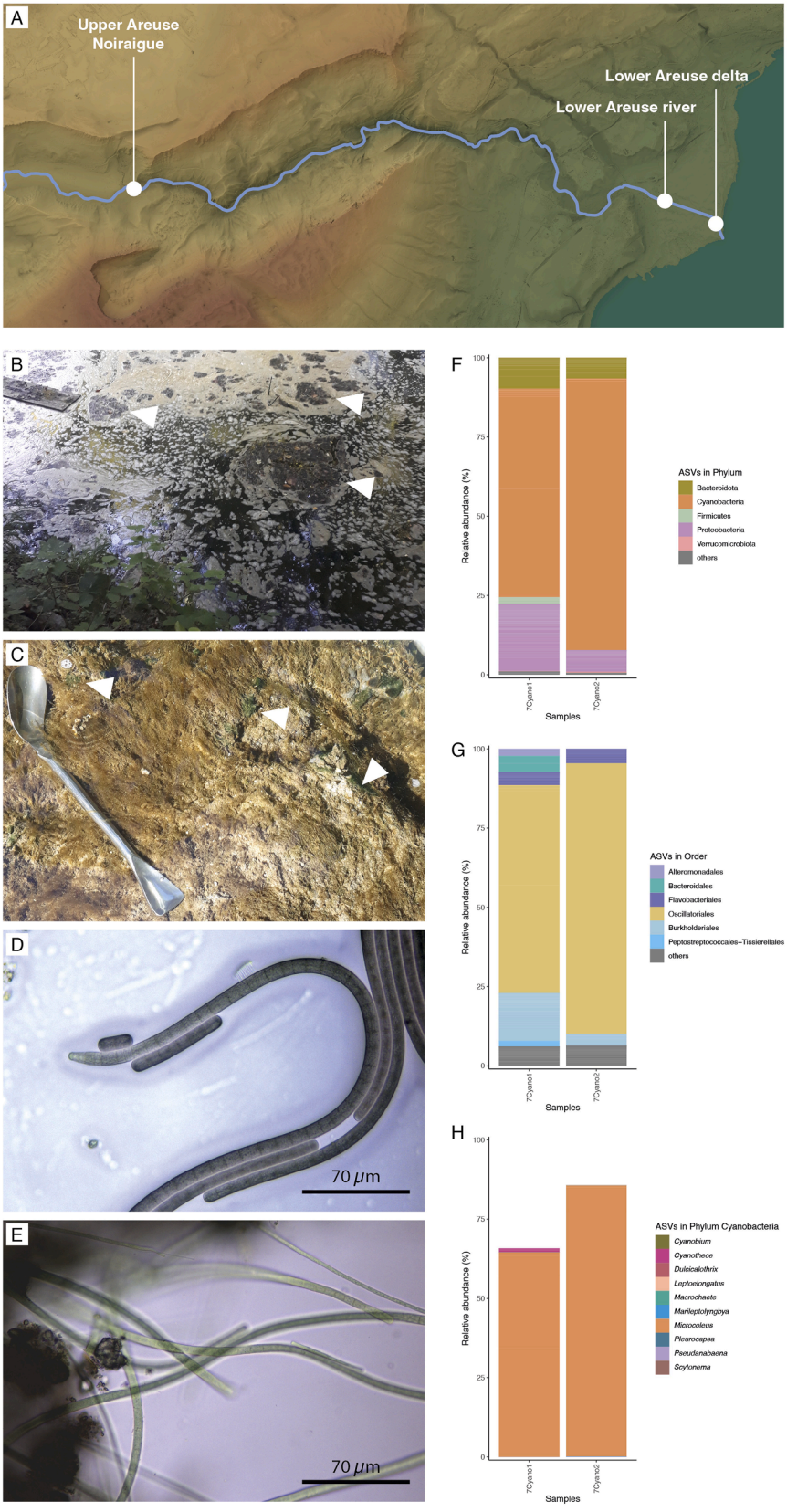

(caption on next page)

Fig. 1. The initial toxigenic bloom event (July-August 2020). A. Map of the main sampling sites along the Areuse (Federal Office of Topography *swisstopo*). B. Mats and scum (mixed mats and pollen) accumulating at the surface of the river close to the mouth of the Areuse. The low level of the river and a backflow of Lake Neuchâtel created an area of low flow and accumulation of biomass in which floating mats were clearly observed. Arrows indicate the floating mats. C. Benthic mats on stones with bright green patches (arrows) dominated by *Potamolinea* sp. D. Trichomes composing the toxigenic mats collected close to the mouth of the Areuse (dominant species: *Microcoleus* sp.). These trichomes lack branching, heterocysts, and akinetes, and are characteristic of Oscillatoriales. Phase contrast microscopy, objective 100x. E. Trichomes composing the bright green mats collected close to the mouth of the Areuse (dominant species: *Potamolinea* sp.). Phase contrast microscopy, objective 100x. F. and G. The composition of the bacterial communities in the floating mats collected close to the mouth of the Areuse at Phylum (F) and the Order (G) levels. The communities present in two samples were analyzed on the basis of the V3-V4 region of the 16S rRNA gene. H. The cyanobacterial fraction of the bacterial community is clearly dominated by *Microcoleus* at the genus level.<AuQuery: Please check,Part designations in figure legends should be in normal typeface (not bold face).>

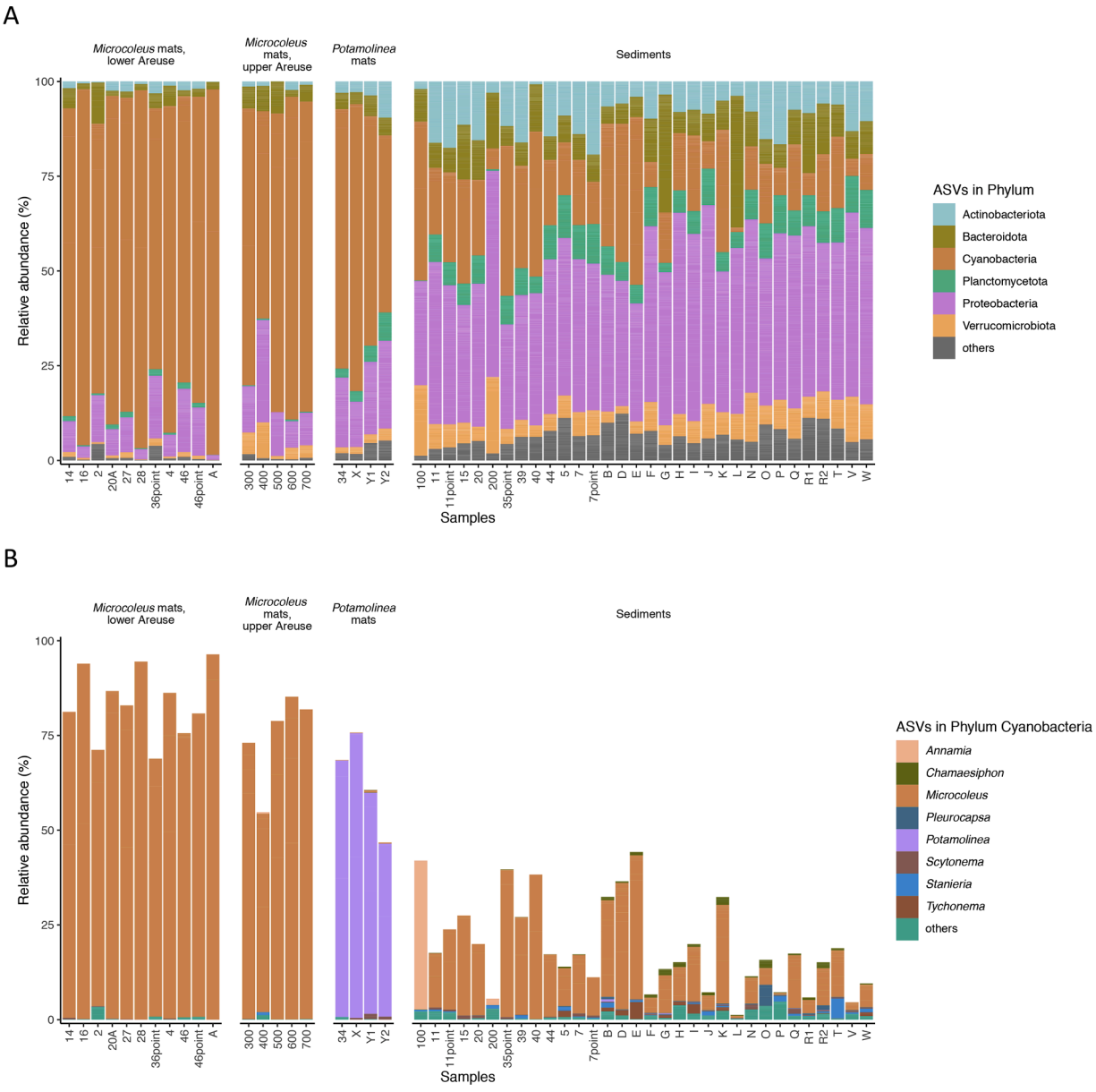

Fig. 2. Composition of the bacterial communities present in mats and sediments from the Areuse in September 2020. The community composition is based on the V3-V4 region of the 16S rRNA gene. The samples have been arranged by type (cyanobacterial mats vs sediments), dominant species (*Microcoleus* vs *Potamolinea*) and, for mats, by location (Lower Areuse vs Upper Areuse / Noiraigue). A. Community analysis at the phylum level, showing a substantial presence of Cyanobacteria and Proteobacteria in collected mats and sediments. B. Community analysis at the genus level, showing the dominance of *Microcoleus* in the cyanobacterial fraction of most samples.

identity [ANI]). Based on a set of 28 conserved protein sequences, the NeuA strain formed a monophyletic clade with the ATX-producing strains from the USA and New Zealand (Fig. 3B, SFigure 7) and showed high conservation over the 16S rRNA gene (>98 % identity; SFigure 7). ANI with strains from the USA, New Zealand, and Canada was always above 0.94 and in most cases above 0.95, the original species threshold (Fig. 3C) (Richter and Rosselló-Móra, 2009). The Aligned Fraction (AF, SFigure 8) for predicted genes was in general above 50 %,

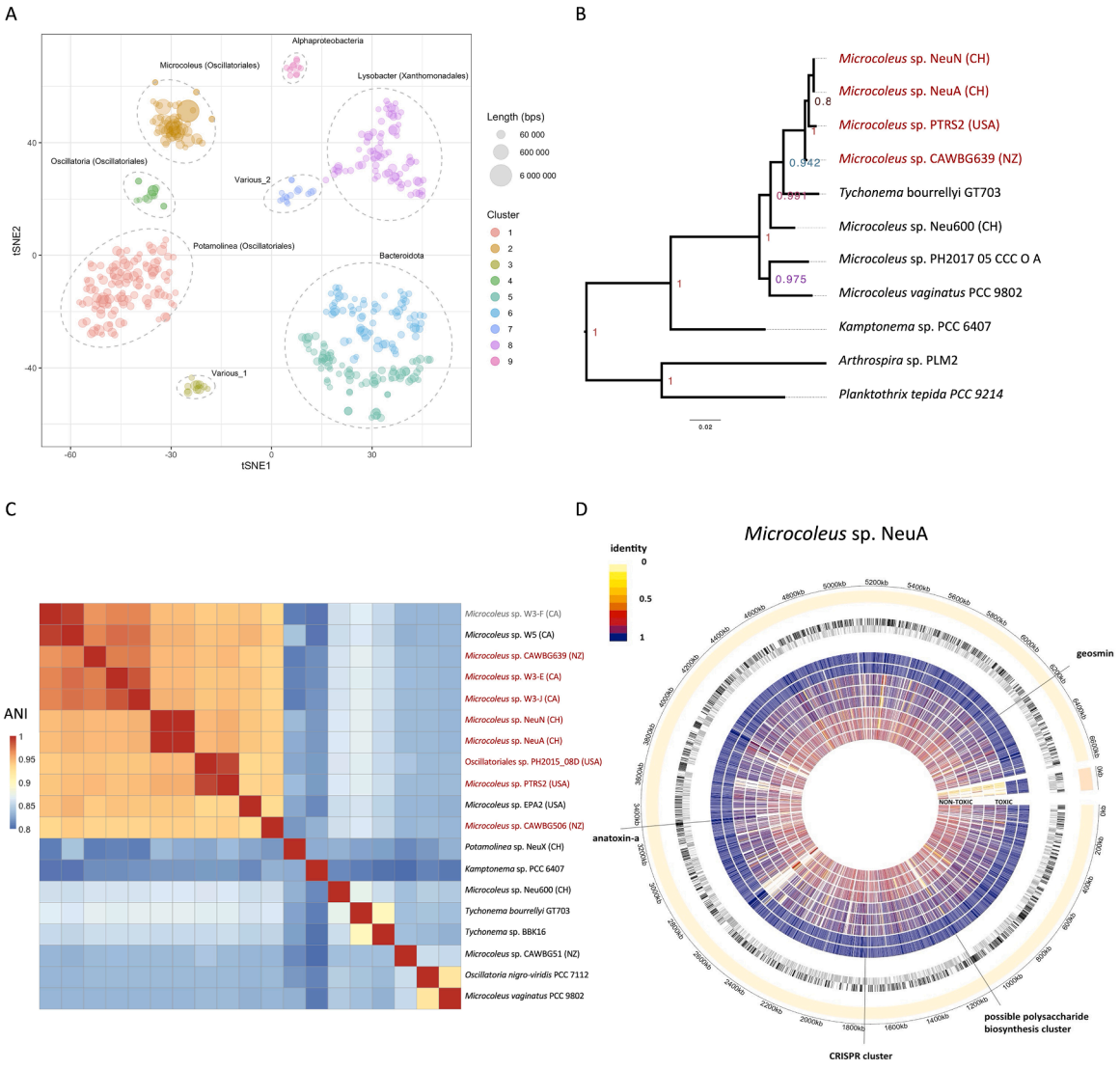

Fig. 3. Phylogenomic characteristics of *Microcoleus* strains isolated from the Areuse. A. Clustering of metagenomic contigs obtained from samples A, N, 600, and X, showing two main clusters of Oscillatoriales (*Microcoleus* and *Potamolinea*) and several clusters of associated heterotrophs (mainly proteobacteria and bacteroidota). The graph is the result of a tSNE clustering of the contigs based on pentanucleotide frequencies. Different predicted clusters are distinguished by color and labelled according to the dominant taxonomic group. The two largest overlapping circles in the *Microcoleus* cluster correspond to *Microcoleus anatoxicus* strain NeuA and NeuN. B. Phylogenetic tree of strains closely related to *Microcoleus* sp. NeuA based on 28 conserved proteins. The tree shows that dhATX-synthesizing strains from New-Zealand, the USA, and Switzerland belong to the same clade; *Microcoleus* sp. Neu600 branches before the acquisition of the dhATX biosynthesis cluster. Strains in red contain the ATX biosynthesis cluster. C. Average nucleotide identity (ANI) among strains closely related to *Microcoleus* sp. NeuA. The figure indicates that NeuA/N (Switzerland), CAWBG639 (New Zealand), PTRS2 (USA), and four strains from the Wolastoq river (Canada) likely belong to the same strain cluster (ANI≥0.94). Both phylogeny and ANI suggest *Tychonema bourrellyi* GT703 and *Microcoleus* sp. Neu600 are the closest relatives of the dhATX-cluster encoding clade. The strain names are colored in red when the ATX biosynthesis cluster was detected among the contigs (ATX positive), in black when the genomic region where the ATX biosynthesis operon should be found was empty (ATX negative), and in grey when the genomic region where the ATX biosynthesis operon should found be was not detected (dubious). D. Circular plot of *Microcoleus* sp. NeuA genome. From the exterior to the interior: a. molecules (yellow: genome; orange: plasmid) and coordinates; b. open reading frames (black: + strand; grey: strand); c. protein identity value between reference (*Microcoleus* sp. NeuA) and *Microcoleus* sp. NeuA (toxic), NeuN (toxic), PTRS1 (toxic), CAWBG639 (toxic), EPA2 (lost dhATX cluster), Neu600 (nontoxic), CAWBG58 (nontoxic), PH2017_15_JOR_U_A (nontoxic), PCC 7112 (nontoxic).

but, for some genome pairs, slightly below 60 %, the accepted species threshold (Varghese et al., 2015); however, the ATX-producing *Microcoleus* group showed strong discontinuity (<30 % AF) with other *Microcoleus* or *Tychonema* species. Based on digital DNA-DNA hybridization [dDDH], strain NeuA has a probability higher than 50 % (conservative value) to belong to the same species as representative dhATX/ATX producing strains from New Zealand, the USA, and Canada, including the taxonomic reference *Microcoleus anatoxicus* strain PTRS2 (estimated dDDH between 60 % and 70 %, STable 3) (Conklin et al., 2020; Meier-Kolthoff et al., 2022). Consistent with this, the secondary structure of the D1-D1′ helix of the 16S-23S rRNA genes internal transcribed spacer (ITS) is identical in *Microcoleus* sp. NeuA, *Microcoleus* sp. EPA2, and *Microcoleus anatoxicus* strain PTRS2 (SFigure 9). Overall, this suggests that the most frequently documented dhATX/ATX producing *Microcoleus* strains proliferating in rivers of temperate countries worldwide belong to a cohesive strain cluster around the *Microcoleus anatoxicus* type strain PTRS2. The NeuA genomes significantly differed from the fragmentary genome assembled from sample 600 (Neu600) based on ANI (<90 %) (Fig. 3C), compositional binning (SFigure 1), and full 16S rRNA gene sequence. Phylogenetically, all three strains

belonged to the *Microcoleus-Tychonema* branch of Oscillatoriales.

The genome content of Microcoleus sp. NeuA

The genome of *Microcoleus* sp. NeuA includes one circular chromosome of 6.5 MB and one circular plasmid of 0.1 MB; it encodes 5687 protein-coding genes, 72 tRNAs, and three rRNA operons (Fig. 3D). The strain shares many features with the dhATX-producing strains from the USA and New Zealand. A number of broad features distinguishes them from closely related strains that do not encode the dhATX biosynthesis cluster, in particular the presence of a specific set of CRISPR/Cas proteins and a large cluster of genes of uncertain function (Fig. 3D).

Microcoleus sp. NeuA encodes a full ATX biosynthesis cluster comprising ten genes (Fig. 4A). This cluster includes the short form of the *anaG* gene and the additional *anaK* gene characteristic of organisms that synthesize dhATX as their main toxin congener (Méjean et al., 2016). The complement and order of the genes is similar to the ones found in other dhATX-producing *Microcoleus* strains except for a variable region, between *anaB-G* and *anaK-I* (Fig. 4A). Overall, these results confirm that the major dhATX-producing *Microcoleus* strains worldwide have similar properties including in terms of toxin-synthesis capacity. By contrast, the contigs assembled from sample 600 did not include an ATX biosynthesis cluster, even fragmentary.

A detailed examination of the flanking regions of the ATX biosynthesis cluster and their homologues in the non-toxic strains, clearly shows three different genomic states (Fig. 4B; SFigure 10): i) an ancestral state before the insertion of the ATX biosynthesis cluster, found in *Tychonema bourrellyi* FEM_GT703, *Tychonema* sp. BBK16, and our *Microcoleus* sp. Neu600, but also in *Microcoleus vaginatus, Oscillatoria nigro-viridis* PCC_7112, and in the *Kamptonema* genus; ii) a state where the full cluster is present at the same position, found in *Microcoleus* sp. CAWBG639, PTRS1 and NeuA; and iii) a third state found in *Microcoleus* sp. EPA2 (USA), where most of the cluster has been excised with a leftover of a hundred base pairs, and in *Microcoleus* sp. W3-F (MAG, Canada). The phylogenetic tree in Fig. 4C shows the most likely history of the clade.

Besides the ATX cluster, the genome of *Microcoleus* sp. NeuA encodes biosynthesis clusters homologous with those of geosmin, anachelin (a cyanobacterial siderophore), and scytocyclamide (STable 4). The geosmin cluster is also found in PTRS1 and in other *Microcoleus* strains, whether toxic or not (Churro et al., 2020; Tee et al., 2021). The other two clusters, like many secondary-metabolite biosynthetic clusters in cyanobacteria, are strain-specific.

The dhATX-synthesizing *Microcoleus* strains differ from non-producing *Microcoleus* strains by several genomic traits, in particular a smaller genome size (<7 MB) and the presence of incomplete or alternative metabolic pathways (Tee et al., 2021). The traits reported in these reference genomes hold true for the NeuA Swiss strain. Overall, we find that, compared to nontoxic strains, the dhATX producers tend to lack some genes in vitamin biosynthetic pathways, specifically thiamine (*tenA* coding for thiaminase II), pyridoxal (*pdxH* coding for pyridoxamine 5′-phosphate oxidase), and cobalamine (*cbiG* coding for cobalt-precorrin 5A hydrolase), to have more genes involved in sugar metabolism and polysaccharide modification, as well as lipid and lipopolysaccharide metabolism, and to have a different set of CRISPR-cas9 associated proteins (SFigure 11–13).

Bacterial communities associated to different mat-forming cyanobacteria are distinct

Literature suggests that ATX-producing *Microcoleus* strains harbor specific cyanosphere-associated bacteria (Bouma-Gregson et al., 2019). To test this hypothesis, we did a Non-metric MultiDimensional Scaling (NMDS) ordination at the species level on the mat datasets, excluding all cyanobacterial ASVs. Samples dominated by *Microcoleus* sp. NeuA, *Microcoleus* sp. Neu600, and *Potamolinea* sp. clustered separately in both a Bray-Curtis dissimilarity-based NMDS ordination (Fig. 5A) and a UniFrac-based NMDS ordination (SFigure 14). Among the most abundant taxa present in the samples, sphingobacteriales —*Pedobacter, Paludibacter*, and *Flavobacterium*— and proteobacteria —Rhodobacteraceae and *Arenimonas*— are likely to be major contributors to the differences between the three groups of samples (Fig. 5A; SFigure 14). Consistent with these results, *Microcoleus* is positively correlated with the *Pedobacter* genus and negatively correlated with the *Potamolinea* genus (Fig. 5B). A co-occurrence network analysis based on the lower Areuse samples confirms the association between *Microcoleus* sp. NeuA and *Pedobacter* as well as the negative relation between *Microcoleus* sp. NeuA and *Potamolinea* (Fig. 5C). Overall, these results strongly suggest that the bacterial communities assembled around different mat-forming cyanobacteria present a different composition.

Discussion

The dog poisoning event that happened in July 2020 by the lake Neuchâtel adds to an increasing list of episodes of intoxications due to benthic cyanobacteria (Svircev et al., 2019; Wood et al., 2020). Similar ATX-associated benthic proliferations have been documented in different rivers in France, Germany, New Zealand, the USA, and Canada,

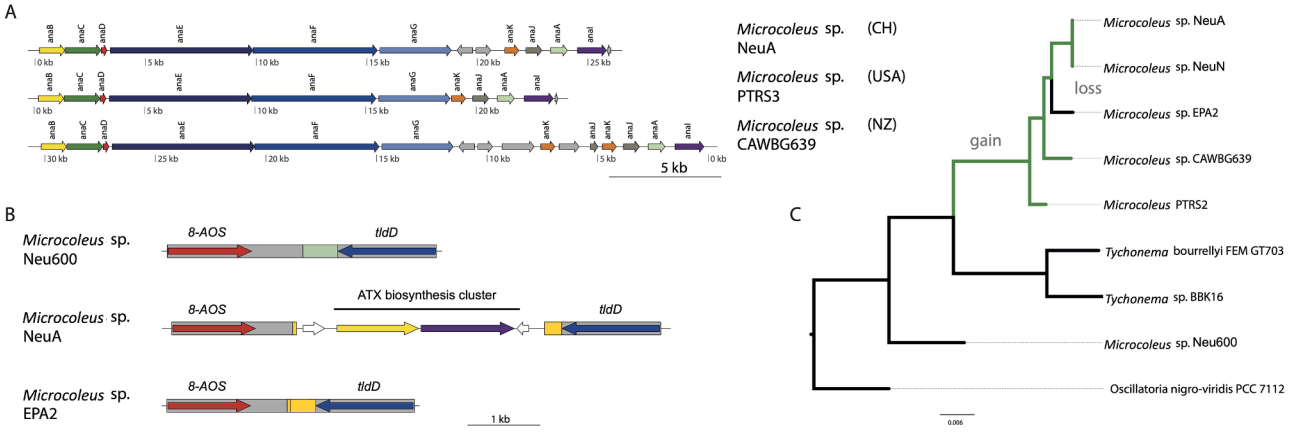

Fig. 4. Sequence and evolution of the dhATX biosynthesis cluster in *Microcoleus* species. A. dhATX biosynthetic clusters from *Microcoleus* sp. NeuA, PTRS1 (USA), and CAWBG639 (NZ). The clusters are very conserved except for a variable region between the two parts of the cluster (*anaBCDEFG* and *anaKJAI*). B. The genomic context of the dhATX cluster in the ancestral nontoxic state (Neu600), after dhATX cluster acquisition (NeuA), and after secondary loss (EPA2). In green, a portion of DNA found in the ancestral state only; in orange, a portion of the dhATX biosynthesis cluster, which remains in EPA2 after cluster loss. C. Reconstruction of gain and loss events on a phylogenetic tree.

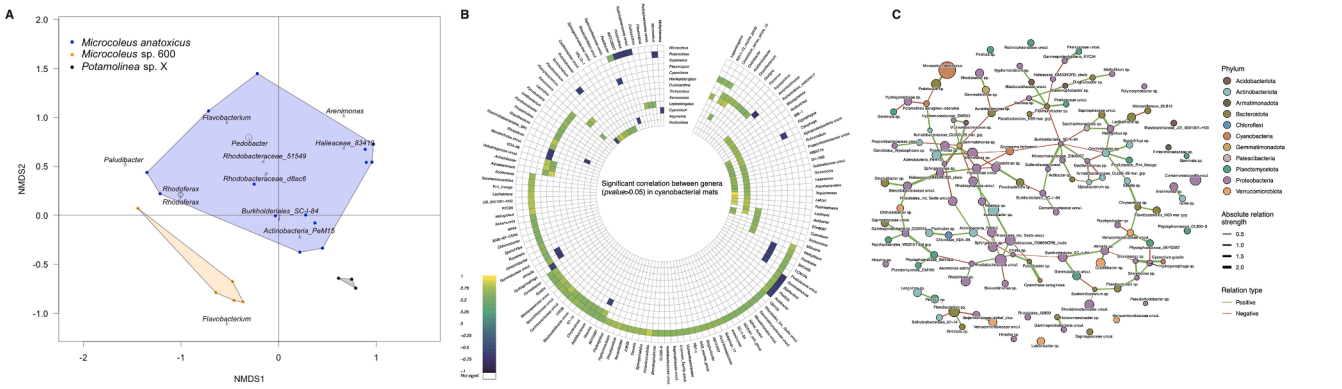

Fig. 5. Bacterial communities in benthic mats differ in composition depending on the dominant cyanobacterial species. A. Non-metric MultiDimensional (NMDS) ordination based on Bray-Curtis distances of bacterial communities in mat samples excluding all cyanobacterial ASVs (species level). All samples in the three first groups shown in Fig. 2 are represented colored by the dominant cyanobacterium (*Microcoleus* sp. NeuA and sp. Neu600, *Potamolinea* sp.). The two first dimensions of the NMDS are sufficient to separate the three groups of associated bacterial communities, which suggests that the communities are distinct from one another. The 12 most common species in the communities are mapped onto the ordination space; the diameter of the open point that represents them is proportional to their mean abundance. B. Significant correlations (Spearman, p-value < 0.05) between cyanobacterial genera and all bacterial genera represented in more than two samples (mats only). C. Co-occurrence network reconstruction from the mat samples (excluding the upper Areuse mats), showing that the toxigenic *Microcoleus* species presents positive co-occurrence with *Pedobacter* sp. and negative co-occurrence with *Potamolinea* sp. Nodes are colored by Phylum; edge color indicates positive or negative co-occurrence; edge width represents co-occurrence strength.

among others, over the last 20 years (Bauer et al., 2020; Fastner et al., 2018; McAllister et al., 2018; Shams et al., 2015; Tee et al., 2021; Valadez-Cano et al., 2023). In all these events, the photosynthetic mats often contained a mixture of toxic and nontoxic benthic Oscillatoriales, with at least one strain being assigned to the genera *Microcoleus, Phormidium,* or *Tychonema.* Because of the confusion surrounding Oscillatoriales taxonomy and the limitations of 16S rRNA-based phylogenies, it has been difficult to assess how closely related toxic and nontoxic benthic cyanobacterial strains were within a bloom and across blooms (Conklin et al., 2020; Kelly et al., 2018, 2019; Tee et al., 2021, 2020; Valadez-Cano et al., 2023). In addition, since cyanotoxin biosynthesis clusters are known to transfer horizontally among Cyanobacteria (Dittmann et al., 2013; Leikoski et al., 2009), it has been unclear whether the benthic Oscillatoriales that produced ATX worldwide were phylogenetically diverse or members of a cohesive phylogenetic cluster (e.g. species). Here, we extend the efforts of recent research endeavors to clarify this question using genome-wide analyses (Conklin et al., 2020; Tee et al., 2021; Valadez-Cano et al., 2023).

Because we used long-read metagenomics, we were able to assemble a full circular genome of the dominant toxic strain responsible for the bloom in the Areuse, ensuring that the genome represents a single strain rather than a mixture of closely related strains. Strain NeuA is closely related to *M. anatoxicus* strain PTRS2, based on a conserved protein phylogeny, the 16S rRNA gene sequence (99.07 % identity), the average nucleotide identity (ANI: 96.04 %) of aligned regions and the aligned fraction (AF: 63.4 %) of the chromosome (digital DNA-DNA hybridization [dDDH] (61.6–67.4 %, recommended method), and structure of the D1-D1′ helix of the ITS between the 16S and 23S rRNA genes (Fig. 3, SFigure 6–9). Except for dDDH, which is slightly lower than the usually accepted 70 % species threshold, all other criteria support the classification of the strain sequenced from the Areuse as *Microcoleus anatoxicus* strain NeuA. Moreover, other dhATX- or ATX-producing *Microcoleus* strains from New Zealand, the USA, and Canada (CAWBG639, CAWBG506, PH2015_08D_45_74, EPA2, and several strains from the Wolastoq river) also belong to the same strain cluster (Fig. 3C, SFigure 8). Although ANI is slightly below the 95 % threshold and AF below the 60 % threshold for a few pairs of strains, there is a large gap between the *M. anatoxicus* strain cluster and the closest strains outside of it (ANI<90 % and AF<30 % in all cases, see Fig. 3C, SFigure 8). This suggests that allele exchange is high within the *M. anatoxicus*-related strain cluster and much lower with strains outside of it. In our view and according to a broadly-accepted bacterial species concept (Caro-Quintero and Konstantinidis, 2012), this would justify to include all the strains in the cluster within a single species, *M. anatoxicus,* even if some values are slightly below the lower threshold. However, more circular genome sequences and a closer comparative analysis would be needed to fully support this statement.

Most *M. anatoxicus*-related strains encode a variant of the ATX biosynthesis cluster known to generate dhATX as the main toxin congener (Méjean et al., 2016; Tee et al., 2021). Whenever present, the cluster is inserted at the exact same locus, suggesting that these strains share a common ATX-producing ancestor (see Fig. 4C, SFigure 10). Interestingly, a number of strains within the group have lost the ATX operon: it is the case of the EPA2 strain from the USA (Tee et al., 2021) and at least one isolate from the Wolastoq river (W3-F) (See Fig. 3) (Valadez-Cano et al., 2023). This suggests that the ATX biosynthesis cluster might be frequently lost in nature because of its cost, as has been proposed in the literature (Heath et al., 2016), and possibly also because the region where it is inserted is particularly prone to recombination (See Fig. 4C and SFigure 10). The high rearrangement rate in the central part of the cluster and subsequent loss of *anaK* (like in strain PH2015_08_D_45_74, see SFigure 10) may explain why some strains in New Zealand, the USA and Canada were synthesizing ATX (or sometimes HTX) rather than dhATX as the main toxic species (Kelly et al., 2019; Valadez-Cano et al., 2023; Wood et al., 2012).

Photosynthetic benthic mats often are complex assemblages and often contain a mixture of toxic and nontoxic benthic cyanobacteria. In our dataset, for instance, sample 600 was dominated by the nontoxic *Microcoleus* strain Neu600 (based on metagenomics), but tested positive for *anaC*. This suggests that a small proportion of an ATX-producing strain, maybe a close relative of *Microcoleus* strain NeuA, was present in the sample together with the nontoxic strain as has been observed in other blooms (Kelly et al., 2019). Based on the community data, the presence of *Potamolinea* spp. appears to limit the dominance of *Microcoleus* sp. and correlates with low toxin levels. This may hint at potential competition between strains of the two genera.

Microcoleus/Phormidium-associated bacterial communities are thought to be quite similar across countries at higher taxonomic levels (Echenique-Subiabre et al., 2018). In our dataset, however, the bacterial communities assembled around benthic cyanobacteria appear to be species-specific at lower taxonomic levels as well (genus and species) (Fig. 5): closely related species like *M. anatoxicus* strain NeuA/N and

Microcoleus sp. 600, for instance, harbor clearly distinct communities (Fig. 5A). We find that Sphingobacteriales (especially *Pedobacter* in our case) may play a central role in the communities surrounding *M. anatoxicus*. Future studies should address whether the potential vitamin auxotrophies of the dhATX-producing *Microcoleus* strains may be balanced in nature by an association with specific vitamin-producing heterotrophic strains (Tee et al., 2021).

In conclusion, this study shows a clear convergence between cyanotoxic events happening at remote sites on the planet. These events are caused by strains belonging to a cohesive cluster of strains around the *M. anatoxicus* type strain PTRS2 and encoding a biosynthesis operon that usually produces dhATX as main toxic congener. These strains are capable of uncontrolled proliferation during warm seasons, during which their floating mats are a threat to mammals, especially dogs. We recommend that such blooms be reported and that specific management procedures be developed.

Material and methods

Sampling

The sampling sites corresponded to three areas: (1) the mouth of the Areuse river, just before it connects to Lake Neuchâtel; (2) River delta, and (3) by a dam on the river in Noiraigue. The two first samples were taken at the mouth on July 31st, 2020, right after the death of several dogs, and on August 16, 2020, as part of a first monitoring of the evolution of the proliferation. On September 8th, 2020, a sampling campaign took place to establish the extent of the zone where cyanobacterial mats developed in the river and in the lake. The first series of samples came from the river banks, mats or sediments on rocks and other emerged surfaces (23 samples; codes A to Y). In addition, samples from underwater mats and sediments from the river mouth and from the delta were obtained by diving (numerical codes below 100). Finally, on September 11, 2020, a second sampling took place near the town of Noiraigue and included three stations: directly in the town, near an abandoned dam and upstream of the current dam (7 samples; numerical codes 100 and above; Table S1). All samples were collected using a spatula to transfer cyanobacterial mats/biomass into tubes as free of contamination as possible.

DNA extraction

The DNA extraction protocol was adapted from the *MP FastDNA Spin Kit for Soil* (MP Biomedicals, Santa Ana, CA, USA). Briefly, 500 mg of biomass (wet weight) were added to Lysing Matrix E tubes containing MT buffer and vortexed. The tubes were then placed in a Tissue Lyser for 10 min at 50 Hz, with intermittent cooling on ice. After centrifugation to remove debris, the supernatant was transferred to new tubes. For protein precipitation, Protein Precipitation Solution was added to the supernatant. The mixture was left to precipitate at 4 °C for 10 min, followed by centrifugation. The Binding Matrix suspension was added to the supernatant. After incubation, the mixture was filtered through SPIN™ filters; multiple rounds of filtration were conducted if necessary. DNA was eluted from the matrix at 55 °C in 100 µl H2O. Storage was done at −20 °C.

16S rRNA gene PCR for cyanobacteria identification

A 40-cycle polymerase chain reaction (PCR) was performed using specific primers for cyanobacteria, Cya106f (5′-CGG ACG GGT GAG TAA CGC GTG A-3′) and Cya781R(b) (5′-GAC TAC AGG GGT ATC TAA TCC CCT T-3′) (Nübel et al., 1997) with the AllinTM Red Taq DNA Polymerase (highQu GmbH, Kraichtal, Germany). Annealing temperature was 58 °C. The amplicon was sequenced using the Sanger method (Microsynth A.G., Switzerland). The amplified DNA was then purified by depositing the PCR products in a 96-well MultiScreen PCR plate (Millipore). A vacuum of 15 inHg was applied to the wells containing the PCR products until all the wells were dry (12–15 min). 30 µl of sterile ultrapure water was added to the wells, which were then allowed to stand for 1 min. The samples were resuspended in ultrapure water by back and forth pipetting and transferred to Eppendorfs with a volume of 0.5 ml. Purified PCR products were quantified again using the Qubit fluorometer before being sent to Fasteris for Sanger sequencing. Each PCR product was sequenced in both directions. After sequencing, each sample had a forward sequence and a reverse sequence. These sequences were then compared to a database available online (GenBank®) using the NCBI Basic Local Alignment Tool (BLAST) web interface (Johnson et al., 2008).

16S rRNA gene community sequencing

The V3-V4 region (universal primers Bakt_341F 5′-CCT ACG GGN GGC WGC AG-3′ and Bakt_805R 5′-GAC TAC HVG GGT ATC TAA TCC-3′) (Herlemann et al., 2011) was amplified with a sample barcoding to allow multiplexing and adapter ligation to enable sequencing on the Illumina MiSeq platform (2 × 300 bp paired end reads). Demultiplexed and trimmed sequence reads provided by Fasteris were processed using *QIIME2* (Bolyen et al., 2019) with *dada2* (Callahan et al., 2016) for the denoising step. Reads were truncated to 478 bases, the optimal length based of q-scores; a minimal overlap of at least 12 identical bases between pair-end reads was required to build a full sequence. The sequences were taxonomically classified using *QIIME2*'s *VSEARCH*-based consensus taxonomy classifier (Rognes et al., 2016) with the *Silva* database (Quast et al., 2012), release 138, for 16S rRNA genes. The Silva database was fine-tuned using the RESCRIPt QIIME2 plugin (Robeson et al., 2021), provided by the QIIME2 Team. Once the ASVs were determined, all ASVs represented in the template-free control samples were excluded from the corresponding culture collection. The co-occurrence network analysis was performed using *SpiecEasi* (Kurtz et al., 2015).

Pacific biosciences (Pacbio) SMRT shotgun metagenomics

1 µg DNA extracted from four environmental samples (A, N, 600, X) was used to prepare standard bacterial Pacbio sequencing libraries (insert size: 9000 bps), Libraries were purified using Ampure beads and bound using Sequel® II Binding Kit 2.2. The libraries were sequenced on a Sequel II instrument as part of a 6-sample multiplexed run. Read count per sample was between 166′000 and 345′000, base count between 600 M and 1800 M. High fidelity reads were generated using Pacbio CCS.

Genome assemblies

Genome assemblies were generated from high-fidelity reads only using *flye* (v. 2.9.2) with the –pacbio-hifi, –meta and –min-overlap 1000 options and three rounds of polishing; assemblies were further polished using *racon* (v. 1.5.0) with default parameters; *dnaA* (genome) and *parA* (plasmids) homologs were used to fix the start of circular genomes using *circlator* (v. 1.5.5). Contigs were assigned to taxonomical categories using *kraken2* (online version on the bv-brc.org website). Contigs larger than 20kbps were binned using *Rtsne* (pca=TRUE, perplexity=5, theta=0.1, check_duplicates = *F*) based on average observed over expected pentanucleotide frequency values calculated based on an in-house script. Coverage values were derived from *flye* assembly reports. Average Nucleotide Identity and alignment lengths were calculated using the *pyani* script (https://github.com/widdowquinn/pyani) on full genomes / MAGs. Aligned Fraction (AF) was calculated on *prodigal* (v. 2.6.3)-predicted coding sequences using *skani* (v. 0.2.1) (Hyatt et al., 2010; Shaw and Yu, 2023). 16S rRNA gene comparisons were done using the *pid* function ("PID2" method) of the *Biostrings* R package (H. Pagès, 2017). Digital DNA-DNA hybridization was carried out using the GGDC 3.0 with Formula 2 (identities / HSP length) (https://ggdc.dsmz.

de/) (Meier-Kolthoff et al., 2022). D1-D1′ helix folding prediction was carried out using the *RNAfold* web server (ViennaRNA Package, v. 2.6.4) (Lorenz et al., 2011).

Gene prediction and annotation

Standard annotation was carried out through the NCBI Prokaryotic Genome Annotation Pipeline (PGAP). Protein classification and pathway analyses were done using both the Kyoto Encyclopedia of Genes and Genomes (KEGG) online service (*blastKOALA*) and the comparative systems analysis of the BV-BRC website. The genomes used for comparisons were the following: *Oscillatoria_nigro-viridis* PCC_7112 (GCA_000317475.1), *Tychonema* sp. BBK16 (GCA_021648855.1), *Tychonema bourrellyi* FEM_GT703 (GCA_002412335.2), *Microcoleus* sp. CAWBG58 (GCA_020883045.1), *Microcoleus* sp. PH2017_15_JOR_U_A (GCA_020738445.1), *Microcoleus* sp. EPA2 (GCA_020882975.1), *Microcoleus* sp. CAWBG639 (GCA_020883025.1). For American *Microcoleus* strains PTRS1–3 (SRR10997082–4) and Canadian *Microcoleus* sequences (W3-F: SRR21374384, W3-E: SRR21374385, W5: SRR21374391, W3-J: SRR21374397), contigs were assembled from traces using *metaspades* (v. 3.15.5) with standard options. Proteome comparisons were carried out using the Proteome comparison service of BV-BRC (*Microcoleus* sp. strain A or *Oscillatoria nigro-viridis* PCC 7112 as reference proteomes) and plotted on the reference genome using the *circlize* R library. The secondary metabolite biosynthesis clusters were predicted using the online *antiSMASH* service.

Phylogenetic trees

356 complete cyanobacterial genomes (nucleotides, proteomes, and annotations) were downloaded from NCBI. Large protein-based phylogenetic trees were built using *fasttree* with -wag and -gamma options from a multiple alignment, made using *muscle* or *kalign* with default parameters, of 28 concatenated conserved proteins (essentially ribosomal proteins). Large 16S rRNA phylogenetic trees were built using *fasttree* with -gtr option from a multiple alignment made using *muscle* with default parameters. A phylogenetic tree based on 28 concatenated conserved proteins for strains close to *Microcoleus anatoxicus* was built using *iqtree2* with automated optimization of the transition matrix; alignment was made using *muscle*.

Plots and figures

Figures were made using *R* (v. 3.14). The following *R* libraries were used: *ggplot2, pheatmap, circlize, biostrings, igraph*.

Analysis of anatoxin-a and dihydroanatoxin-a

The sample collected in early August was analyzed by Ultra-high-performance liquid chromatography (UHPLC) coupled with a high-resolution mass spectrometer (HR-MS) (Müller et al., 2022). The samples collected in September (STable 1) were analyzed using a UHPLC coupled with a triple quadrupole MS (TQMS) and with a selected reaction monitoring strategy for ATX as published previously (Turner et al., 2022). Briefly, the cyanobacteria samples were centrifuged (30 min, 4000 g) and the supernatant was discarded. Water (30 mL) was added to the biomass, the mixture was vortexed and centrifuged (30 min, 4000 g), and the solution was decanted and discarded. An aqueous MeOH soln. (30 mL, 50 %) was added to the biomass, the mixture was sonicated (3 × 3 min), centrifuged (30 min, 4000 g), and the supernatant was collected and dried under a gentle flow of nitrogen. An aqueous MeOH soln. (50 %) was added to the samples to afford a concentration of 1 mg/mL of extract and the samples were directly analyzed by UHPLC-ESI-MS in positive mode (Ultimate 3000 LC, Thermo Fisher Scientific, coupled to a TSQ Quantum Ultra, Thermo Fisher Scientific). The column used was the Kinetex Polar C18 (50 × 2.1 mm, 2.6 μm), the flow rate was set up to 0.4 ml/min, the column oven temperature was at 40 °C, and the solvent system used was composed of A (H_2O with 0.1 % HCO_2H) and B (MeCN with 0.1 % HCO_2H). The column was pre-equilibrated with 0 % B for 1 min, the gradient increased to 60 % B over 3.5 min and to 100 % over 0.05 min, and was kept to 100 % B for 1.24 min. The detection was achieved using the SRM mode as previously reported (Turner et al., 2022) and a fragmentation from 166.2 to 130 was selected. For the quantification of dihydroanatoxin-a, the calibration curve was based on the SIM of anatoxin-a at 166.2 m/z and the concentration of dihydroanatoxin-a in the sample was calculated using the SIM mode at 168.2 m/z. The quantification was done using a calibration curve obtained using analytical standard solutions prepared with the commercially available anatoxin fumarate (Bio-Techne).

CRediT authorship contribution statement

Pilar Junier: Writing – review & editing, Writing – original draft, Visualization, Validation, Supervision, Resources, Project administration, Methodology, Investigation, Funding acquisition, Conceptualization. **Guillaume Cailleau:** Writing – review & editing, Visualization, Methodology, Investigation, Formal analysis, Data curation. **Mathilda Fatton:** Writing – review & editing, Investigation. **Pauline Udriet:** Writing – review & editing, Investigation. **Isha Hashmi:** Writing – review & editing, Investigation. **Danae Bregnard:** Writing – review & editing, Investigation. **Andrea Corona-Ramirez:** Writing – review & editing, Investigation. **Eva di Francesco:** Writing – review & editing, Investigation. **Thierry Kuhn:** Writing – review & editing, Investigation. **Naïma Mangia:** Writing – review & editing, Investigation. **Sami Zhioua:** Writing – review & editing, Investigation. **Daniel Hunkeler:** Writing – review & editing, Investigation. **Saskia Bindschedler:** Writing – review & editing, Investigation. **Simon Sieber:** Writing – review & editing, Writing – original draft, Validation, Resources, Methodology, Investigation, Formal analysis, Data curation, Conceptualization. **Diego Gonzalez:** Writing – review & editing, Writing – original draft, Visualization, Validation, Software, Methodology, Investigation, Formal analysis, Data curation, Conceptualization.

Declaration of competing interest

The authors declare the following financial interests/personal relationships which may be considered as potential competing interests:

Diego Gonzalez reports financial support was provided by Swiss National Science Foundation. If there are other authors, they declare that they have no known competing financial interests or personal relationships that could have appeared to influence the work reported in this paper.

Data availability

Metagenome-assembled genome sequences were deposited on the NCBI repository under bioproject PRJNA943188. 16S rRNA data were deposited NCBI under bioproject PRJNA1125304.

Acknowledgments

We thank Daniel Borel and Nathan Villat for their help during the sampling campaign, as well as Céline Terrettaz for follow up work. D.G's work was supported by the Swiss National Science Foundation (PZ00P3_180142 to D.G., 2020–2023) and the *Velux Foundation* (grant 1814 to P.J. and D.G., 2023).

Supplementary materials

Supplementary material associated with this article can be found, in the online version, at doi:10.1016/j.wroa.2024.100252.

References

Bauer, F., Fastner, J., Bartha-Dima, B., Breuer, W., Falkenau, A., Mayer, C., Raeder, U., 2020. Mass Occurrence of Anatoxin-a- and Dihydroanatoxin-a-Producing Tychonema sp. in Mesotrophic Reservoir Mandichosee (River Lech, Germany) as a Cause of Neurotoxicosis in Dogs. Toxins. (Basel) 12, 726. https://doi.org/10.3390/toxins12110726.

Bolyen, E., Rideout, J.R., Dillon, M.R., Bokulich, N.A., Abnet, C.C., Al-Ghalith, G.A., Alexander, H., Alm, E.J., Arumugam, M., Asnicar, F., Bai, Y., Bisanz, J.E., Bittinger, K., Brejnrod, A., Brislawn, C.J., Brown, C.T., Callahan, B.J., Caraballo-Rodríguez, A.M., Chase, J., Cope, E.K., Da Silva, R., Diener, C., Dorrestein, P.C., Douglas, G.M., Durall, D.M., Duvallet, C., Edwardson, C.F., Ernst, M., Estaki, M., Fouquier, J., Gauglitz, J.M., Gibbons, S.M., Gibson, D.L., Gonzalez, A., Gorlick, K., Guo, J., Hillmann, B., Holmes, S., Holste, H., Huttenhower, C., Huttley, G.A., Janssen, S., Jarmusch, A.K., Jiang, L., Kaehler, B.D., Kang, K.B., Keefe, C.R., Keim, P., Kelley, S.T., Knights, D., Koester, I., Kosciolek, T., Kreps, J., Langille, M.G.I., Lee, J., Ley, R., Liu, Y.X., Loftfield, E., Lozupone, C., Maher, M., Marotz, C., Martin, B.D., McDonald, D., McIver, L.J., Melnik, A.V., Metcalf, J.L., Morgan, S.C., Morton, J.T., Naimey, A.T., Navas-Molina, J.A., Nothias, L.F., Orchanian, S.B., Pearson, T., Peoples, S.L., Petras, D., Preuss, M.L., Pruesse, E., Rasmussen, L.B., Rivers, A., Robeson, M.S., Rosenthal, P., Segata, N., Shaffer, M., Shiffer, A., Sinha, R., Song, S.J., Spear, J.R., Swafford, A.D., Thompson, L.R., Torres, P.J., Trinh, P., Tripathi, A., Turnbaugh, P.J., Ul-Hasan, S., Van Der Hooft, J.J.J., Vargas, F., Vázquez-Baeza, Y., Vogtmann, E., Von Hippel, M., Walters, W., Wan, Y., Wang, M., Warren, J., Weber, K.C., Williamson, C.H.D., Willis, A.D., Xu, Z.Z., Zaneveld, J.R., Zhang, Y., Zhu, Q., Knight, R., Caporaso, J.G., 2019. Reproducible, interactive, scalable and extensible microbiome data science using QIIME 2. Nat. Biotechnol. 37, 852–857. https://doi.org/10.1038/s41587-019-0209-9.

Bouma-Gregson, K., Kudela, R.M., Power, M.E., 2018. Widespread anatoxin-a detection in benthic cyanobacterial mats throughout a river network. PLoS. One 13, e0197669. https://doi.org/10.1371/journal.pone.0197669.

Bouma-Gregson, K., Olm, M.R., Probst, A.J., Anantharaman, K., Power, M.E., Banfield, J. F., 2019. Impacts of microbial assemblage and environmental conditions on the distribution of anatoxin-a producing cyanobacteria within a river network. ISMe J. 13, 1618–1634. https://doi.org/10.1038/s41396-019-0374-3.

Cadel-Six, S., Peyraud-Thomas, C., Brient, L., De Marsac, N.T., Rippka, R., Méjean, A., 2007. Different Genotypes of Anatoxin-Producing Cyanobacteria Coexist in the Tarn River, France. Appl. Environ. Microbiol. 73, 7605–7614. https://doi.org/10.1128/AEM.01225-07.

Callahan, B.J., McMurdie, P.J., Rosen, M.J., Han, A.W., Johnson, A.J.A., Holmes, S.P., 2016. DADA2: High-resolution sample inference from Illumina amplicon data. Nat. Methods 13, 581–583. https://doi.org/10.1038/nmeth.3869.

Caro-Quintero, A., Konstantinidis, K.T., 2012. Bacterial species may exist, metagenomics reveal. Environ. Microbiol. 14, 347–355. https://doi.org/10.1111/j.1462-2920.2011.02668.x.

Carpine, R., Sieber, S., 2021. Antibacterial and antiviral metabolites from cyanobacteria: Their application and their impact on human health. https://doi.org/10.5167/UZH-221120.

Churro, C., Semedo-Aguiar, A.P., Silva, A.D., Pereira-Leal, J.B., Leite, R.B., 2020. A novel cyanobacterial geosmin producer, revising GeoA distribution and dispersion patterns in Bacteria. Sci. Rep. 10, 8679. https://doi.org/10.1038/s41598-020-64774-y.

Colas, S., Marie, B., Lance, E., Quiblier, C., Tricoire-Leignel, H., Mattei, C., 2021. Anatoxin-a: Overview on a harmful cyanobacterial neurotoxin from the environmental scale to the molecular target. Environ. Res. 193, 110590 https://doi.org/10.1016/j.envres.2020.110590.

Conklin, K.Y., Stancheva, R., Otten, T.G., Fadness, R., Boyer, G.L., Read, B., Zhang, X., Sheath, R.G., 2020. Molecular and morphological characterization of a novel dihydroanatoxin-a producing Microcoleus species (cyanobacteria) from the Russian River, California, USA. Harmful. Algae 93, 101767. https://doi.org/10.1016/j.hal.2020.101767.

Dittmann, E., Fewer, D.P., Neilan, B.A., 2013. Cyanobacterial toxins: biosynthetic routes and evolutionary roots. FEMS Microbiol. Rev. 37, 23–43. https://doi.org/10.1111/j.1574-6976.2012.12000.x.

Echenique-Subiabre, I., Zancarini, A., Heath, M.W., Wood, S.A., Quiblier, C., Humbert, J. F., 2018. Multiple processes acting from local to large geographical scales shape bacterial communities associated with Phormidium (cyanobacteria) biofilms in French and New Zealand rivers. Sci. Rep. 8, 14416. https://doi.org/10.1038/s41598-018-32772-w.

Fastner, J., Beulker, C., Geiser, B., Hoffmann, A., Kröger, R., Teske, K., Hoppe, J., Mundhenk, L., Neurath, H., Sagebiel, D., Chorus, I., 2018. Fatal Neurotoxicosis in Dogs Associated with Tychoplanktic, Anatoxin-a Producing Tychonema sp. in Mesotrophic Lake Tegel, Berlin. Toxins. (Basel) 10, 60. https://doi.org/10.3390/toxins10020060.

Ferrão-Filho, A.da S., Kozlowsky-Suzuki, B., 2011. Cyanotoxins: Bioaccumulation and Effects on Aquatic Animals. Mar. Drugs 9, 2729–2772. https://doi.org/10.3390/md9122729.

Gugger, M., Lenoir, S., Berger, C., Ledreux, A., Druart, J.C., Humbert, J.F., Guette, C., Bernard, C., 2005. First report in a river in France of the benthic cyanobacterium Phormidium favosum producing anatoxin-a associated with dog neurotoxicosis. Toxicon. 45, 919–928. https://doi.org/10.1016/j.toxicon.2005.02.031.

Heath, M., Wood, S.A., RG, Y., Ryan, K.G., 2016. The role of nitrogen and phosphorus in regulating Phormidium sp. (cyanobacteria) growth and anatoxin production. FEMS. Microbiol. Ecol. 92.

Heath, M.W., Wood, S.A., Ryan, K.G., 2011. Spatial and temporal variability in Phormidium mats and associated anatoxin-a and homoanatoxin-a in two New Zealand rivers. Aquat. Microb. Ecol. 64, 69–79. https://doi.org/10.3354/ame01516.

Herlemann, D.P., Labrenz, M., Jürgens, K., Bertilsson, S., Waniek, J.J., Andersson, A.F., 2011. Transitions in bacterial communities along the 2000 km salinity gradient of the Baltic Sea. ISMe J. 5, 1571–1579. https://doi.org/10.1038/ismej.2011.41.

Hyatt, D., Chen, G.L., LoCascio, P.F., Land, M.L., Larimer, F.W., Hauser, L.J., 2010. Prodigal: prokaryotic gene recognition and translation initiation site identification. BMC. Bioinformatics. 11, 119. https://doi.org/10.1186/1471-2105-11-119.

Janssen, E.M.L., 2019. Cyanobacterial peptides beyond microcystins – A review on co-occurrence, toxicity, and challenges for risk assessment. Water. Res. 151, 488–499. https://doi.org/10.1016/j.watres.2018.12.048.

Johnson, M., Zaretskaya, I., Raytselis, Y., Merezhuk, Y., McGinnis, S., Madden, T.L., 2008. NCBI BLAST: a better web interface. Nucleic. Acids. Res. 36, W5–W9. https://doi.org/10.1093/nar/gkn201.

Kelly, L., Wood, S.A., McAllister, T., Ryan, K., 2018. Development and Application of a Quantitative PCR Assay to Assess Genotype Dynamics and Anatoxin Content in Microcoleus autumnalis-Dominated Mats. Toxins. (Basel) 10, 431. https://doi.org/10.3390/toxins10110431.

Kelly, L.T., Bouma-Gregson, K., Puddick, J., Fadness, R., Ryan, K.G., Davis, T.W., Wood, S.A., 2019. Multiple cyanotoxin congeners produced by sub-dominant cyanobacterial taxa in riverine cyanobacterial and algal mats. PLoS. One 14, e0220422. https://doi.org/10.1371/journal.pone.0220422.

Kurtz, Z.D., Müller, C.L., Miraldi, E.R., Littman, D.R., Blaser, M.J., Bonneau, R.A., 2015. Sparse and Compositionally Robust Inference of Microbial Ecological Networks. PLoS. Comput. Biol. 11, e1004226 https://doi.org/10.1371/journal.pcbi.1004226.

Leikoski, N., Fewer, D.P., Sivonen, K., 2009. Widespread Occurrence and Lateral Transfer of the Cyanobactin Biosynthesis Gene Cluster in Cyanobacteria. Appl. Environ. Microbiol. 75, 853–857. https://doi.org/10.1128/AEM.02134-08.

Lorenz, R., Bernhart, S.H., Höner Zu Siederdissen, C., Tafer, H., Flamm, C., Stadler, P.F., Hofacker, I.L., 2011. ViennaRNA Package 2.0. Algorithms. Mol. Biol. 6, 26. https://doi.org/10.1186/1748-7188-6-26.

McAllister, T.G., Wood, S.A., Atalah, J., Hawes, I., 2018. Spatiotemporal dynamics of Phormidium cover and anatoxin concentrations in eight New Zealand rivers with contrasting nutrient and flow regimes. Sci. Total. Environ. 612, 71–80. https://doi.org/10.1016/j.scitotenv.2017.08.085.

McAllister, T.G., Wood, S.A., Hawes, I., 2016. The rise of toxic benthic Phormidium proliferations: A review of their taxonomy, distribution, toxin content and factors regulating prevalence and increased severity. Harmful. Algae 55, 282–294. https://doi.org/10.1016/j.hal.2016.04.002.

Mehinto, A.C., Smith, J., Wenger, E., Stanton, B., Linville, R., Brooks, B.W., Sutula, M.A., Howard, M.D.A., 2021. Synthesis of ecotoxicological studies on cyanotoxins in freshwater habitats – Evaluating the basis for developing thresholds protective of aquatic life in the United States. Science of The Total Environment 795, 148864. https://doi.org/10.1016/j.scitotenv.2021.148864.

Meier-Kolthoff, J.P., Carbasse, J.S., Peinado-Olarte, R.L., Göker, M., 2022. TYGS and LPSN: a database tandem for fast and reliable genome-based classification and nomenclature of prokaryotes. Nucleic. Acids. Res. 50, D801–D807. https://doi.org/10.1093/nar/gkab902.

Méjean, A., Dalle, K., Paci, G., Bouchonnet, S., Mann, S., Pichon, V., Ploux, O., 2016. Dihydroanatoxin-a Is Biosynthesized from Proline in Cylindrospermum stagnale PCC 7417: Isotopic Incorporation Experiments and Mass Spectrometry Analysis. J. Nat. Prod. 79, 1775–1782. https://doi.org/10.1021/acs.jnatprod.6b00189.

Müller, M.J., Dorst, A., Paulus, C., Khan, I., Sieber, S., 2022. Catch-enrich-release approach for amine-containing natural products. Chem. Commun. 58, 12560–12563. https://doi.org/10.1039/D2CC04905H.

Nübel, U., Garcia-Pichel, F., Muyzer, G., 1997. PCR primers to amplify 16S rRNA genes from cyanobacteria. Appl. Environ. Microbiol. 63, 3327–3332. https://doi.org/10.1128/aem.63.8.3327-3332.1997.

Paerl, H.W., Otten, T.G., 2013. Harmful Cyanobacterial Blooms: Causes, Consequences, and Controls. Microb. Ecol. 65, 995–1010. https://doi.org/10.1007/s00248-012-0159-y.

Pagès, H., 2017. Biostrings. https://doi.org/10.18129/B9.BIOC.BIOSTRINGS.

Puddick, J., Kelly, L.T., Wood, S.A., 2022. Climate change and toxic freshwater cyanobacteria in Aotearoa New Zealand (No. 3765), Cawthron Report. Cawthron, New Zealand.

Quast, C., Pruesse, E., Yilmaz, P., Gerken, J., Schweer, T., Yarza, P., Peplies, J., Glöckner, F.O., 2012. The SILVA ribosomal RNA gene database project: improved data processing and web-based tools. Nucleic. Acids. Res. 41, D590–D596. https://doi.org/10.1093/nar/gks1219.

Quiblier, C., Wood, S.A., Echenique, I., Heath, M., Aurelie, V., Humbert, J.F., 2013. A review of current knowledge on toxic benthic freshwater cyanobacteria - Ecology, toxin production and risk management. Water. Res. 47 https://doi.org/10.1016/j.watres.2013.06.042.

Richter, M., Rosselló-Móra, R., 2009. Shifting the genomic gold standard for the prokaryotic species definition. Proc. Natl. Acad. Sci. U.S.A. 106, 19126–19131. https://doi.org/10.1073/pnas.0906412106.

Robeson, M.S., O'Rourke, D.R., Kaehler, B.D., Ziemski, M., Dillon, M.R., Foster, J.T., Bokulich, N.A., 2021. RESCRIPt: Reproducible sequence taxonomy reference database management. PLoS. Comput. Biol. 17, e1009581 https://doi.org/10.1371/journal.pcbi.1009581.

Rognes, T., Flouri, T., Nichols, B., Quince, C., Mahé, F., 2016. VSEARCH: a versatile open source tool for metagenomics. PeerJ. 4, e2584. https://doi.org/10.7717/peerj.2584.

Shams, S., Capelli, C., Cerasino, L., Ballot, A., Dietrich, D.R., Sivonen, K., Salmaso, N., 2015. Anatoxin-a producing Tychonema (Cyanobacteria) in European waterbodies. Water. Res. 69, 68–79. https://doi.org/10.1016/j.watres.2014.11.006.

Shaw, J., Yu, Y.W., 2023. Fast and robust metagenomic sequence comparison through sparse chaining with skani. Nat. Methods 20, 1661–1665. https://doi.org/10.1038/s41592-023-02018-3.

Sieber, S., Grendelmeier, S.M., Harris, L.A., Mitchell, D.A., Gademann, K., 2020. Microviridin 1777: A Toxic Chymotrypsin Inhibitor Discovered by a Metabologenomic Approach. J. Nat. Prod. 83, 438–446. https://doi.org/10.1021/acs.jnatprod.9b00986.

Strunecký, O., Komárek, J., Johansen, J., Lukešová, A., Elster, J., 2013. Molecular and morphological criteria for revision of the genus Microcoleus (Oscillatoriales, Cyanobacteria). J. Phycol. 49, 1167–1180. https://doi.org/10.1111/jpy.12128.

Svircev, Z., Lalic, D., Bojadzija Savic, G., Tokodi, N., Drobac Backovic, D., Chen, L., J, M., Codd, G.A., 2019. Global geographical and historical overview of cyanotoxin distribution and cyanobacterial poisonings. Arch. Toxicol. 93, 2429–2481.

Svirčev, Z., Lalić, D., Bojadžija Savić, G., Tokodi, N., Drobac Backović, D., Chen, L., Meriluoto, J., Codd, G.A., 2019. Global geographical and historical overview of cyanotoxin distribution and cyanobacterial poisonings. Arch. Toxicol. 93, 2429–2481. https://doi.org/10.1007/s00204-019-02524-4.

Tee, H.S., Waite, D., Payne, L., Middleditch, M., Wood, S., Handley, K.M., 2020. Tools for successful proliferation: diverse strategies of nutrient acquisition by a benthic cyanobacterium. ISMe J. 14, 2164–2178. https://doi.org/10.1038/s41396-020-0676-5.

Tee, H.S., Wood, S.A., Bouma-Gregson, K., Lear, G., Handley, K.M., 2021. Genome Streamlining, Plasticity, and Metabolic Versatility Distinguish Co-occurring Toxic and Nontoxic Cyanobacterial Strains of Microcoleus. mBio 12. https://doi.org/10.1128/mBio.02235-21 e02235-21.

Thomson-Laing, G., Puddick, J., Laroche, O., Fulton, S., Steiner, K., Heath, M.W., Wood, S.A., 2020. Broad and Fine Scale Variability in Bacterial Diversity and Cyanotoxin Quotas in Benthic Cyanobacterial Mats. Front. Microbiol. 11, 129. https://doi.org/10.3389/fmicb.2020.00129.

Turner, A.D., Turner, F.R.I., White, M., Hartnell, D., Crompton, C.G., Bates, N., Egginton, J., Branscombe, L., Lewis, A.M., Maskrey, B.H., 2022. Confirmation Using Triple Quadrupole and High-Resolution Mass Spectrometry of a Fatal Canine Neurotoxicosis following Exposure to Anatoxins at an Inland Reservoir. Toxins. (Basel) 14, 804. https://doi.org/10.3390/toxins14110804.

Valadez-Cano, C., Reyes-Prieto, A., Beach, D.G., Rafuse, C., McCarron, P., Lawrence, J., 2023. Genomic characterization of coexisting anatoxin-producing and non-toxigenic Microcoleus subspecies in benthic mats from the Wolastoq, New Brunswick, Canada. Harmful. Algae 124, 102405. https://doi.org/10.1016/j.hal.2023.102405.

Varghese, N.J., Mukherjee, S., Ivanova, N., Konstantinidis, K.T., Mavrommatis, K., Kyrpides, N.C., Pati, A., 2015. Microbial species delineation using whole genome sequences. Nucleic. Acids. Res. 43, 6761–6771. https://doi.org/10.1093/nar/gkv657.

Wood, S.A., Biessy, L., Puddick, J., 2018. Anatoxins are consistently released into the water of streams with Microcoleus autumnalis-dominated (cyanobacteria) proliferations. Harmful. Algae 80, 88–95. https://doi.org/10.1016/j.hal.2018.10.001.

Wood, S.A., Kelly, L.T., Bouma-Gregson, K., Humbert, J., Laughinghouse, H.D., Lazorchak, J., McAllister, T.G., McQueen, A., Pokrzywinski, K., Puddick, J., Quiblier, C., Reitz, L.A., Ryan, K.G., Vadeboncoeur, Y., Zastepa, A., Davis, T.W., 2020. Toxic benthic freshwater cyanobacterial proliferations: Challenges and solutions for enhancing knowledge and improving monitoring and mitigation. Freshw. Biol. 65, 1824–1842. https://doi.org/10.1111/fwb.13532.

Wood, S.A., Smith, F.M.J., Heath, M.W., Palfroy, T., Gaw, S., Young, R.G., Ryan, K.G., 2012. Within-Mat Variability in Anatoxin-a and Homoanatoxin-a Production among Benthic Phormidium (Cyanobacteria) Strains. Toxins. (Basel) 4, 900–912. https://doi.org/10.3390/toxins4100900.

Zanchett, G., Oliveira-Filho, E., 2013. Cyanobacteria and Cyanotoxins: From Impacts on Aquatic Ecosystems and Human Health to Anticarcinogenic Effects. Toxins. (Basel) 5, 1896–1917. https://doi.org/10.3390/toxins5101896.